annalise

Annalise Enterprise 3.0

Performance Guide

English

Annalise Enterprise Product

Product version: **3.0**

Date of issue: **2022-04-26**

ARTG. No. 343577

ANNALISE-AI PTY LTD
ACN 635 645 260

Level 21, 60 Margaret Street,
Sydney NSW 2000

AUSTRALIA

www.annalise.ai

QualRep Services B.V.
Utrechtseweg 310 - Bldg B42,
NL-6812 AR Arnhem,

THE NETHERLANDS

globalreg@qservegroup.com

New Zealand Sponsor

AA-Med NZ Ltd.
Level 7, 54 Gill Street,
New Plymouth, 4310
NEW ZEALAND

Tel: 0800-440-238

Malaysia Authorised Representative

ARQon Medtech Sdn Bhd
No. 20, Jalan Sasa 4, Taman Gaya, 81800,
Johor
MALAYSIA

info@arqon.com

Registration Number: GA5216421-60402

UK Responsible Person

Qserve Group UK, Ltd. 49 Greek Street
Soho, London W1D 4EG
UNITED KINGDOM

globalreg@qservegroup.com

Indian Voluntary Registration Number

Annali-AUS/I/MD/003060

Annalise Enterprise performance

Overview

This document outlines the product performance of Annalise Enterprise.

For general user information, refer to the *Annalise Enterprise User Guide*.

AUC by findings (CXR)

The following tables include all supported findings for Annalise Enterprise (CXR) in alphabetical order. Each row displays both the finding name and the area under the curve (AUC) mean.

These performance results are based on the dataset used by annalise.ai to evaluate the product. Differences in transfer syntax, demographics, imaging equipment or other variables may result in changes in performance.

CXR findings

Finding	AUC mean
abdominal clips	0.9779
acute clavicle fracture	0.9600
acute humerus fracture	0.9739
acute rib fracture	0.9686
airway stent	0.9689
aortic arch calcification	0.9761
aortic stent	0.9939
atelectasis	0.8819
axillary clips	0.9966
basal interstitial thickening	0.8869
biliary stent	0.9987
breast implant	0.9960
bronchiectasis	0.9278
calcified axillary nodes	0.9777
calcified granuloma (< 5mm)	0.9306
calcified hilar lymphadenopathy	0.8889
calcified mass (> 5mm)	0.9532
calcified neck nodes	0.9324
calcified pleural plaques	0.9803
cardiac valve prosthesis	0.9973
cavitating mass with content	0.9713

continued

CXR findings (cont.)

Finding	AUC mean
cavitating mass(es)	0.9282
cervical flexion	0.9919
chronic clavicle fracture	0.9627
chronic humerus fracture	0.9879
chronic rib fracture	0.9477
clavicle fixation	0.9971
clavicle lesion	0.9652
coronary stent	0.9660
diaphragmatic elevation	0.9337
diaphragmatic eventration	0.9825
diffuse airspace opacity	0.9762
diffuse bullae	0.9683
diffuse fibrotic volume loss	0.9604
diffuse interstitial thickening	0.9381
diffuse lower airspace opacity	0.9326
diffuse nodular / miliary lesions	0.9761
diffuse pleural thickening	0.9625
diffuse spinal osteophytes	0.9811
diffuse upper airspace opacity	0.9777
distended bowel	0.9793
electronic cardiac devices	0.9999
focal airspace opacity	0.8517
gallstones	0.8702
gastric band	0.9743
hiatus hernia	0.9915
hilar lymphadenopathy	0.9365
humeral lesion	0.9757
hyperinflation	0.9644
image obscured	0.9369
in position central line (cvc)	0.9950
in position endotracheal tube (ett)	0.9970
in position nasogastric tube (ngt)	0.9965
in position pulmonary arterial catheter (pac)	0.9918
incompletely imaged chest	0.9752

continued

CXR findings (cont.)

Finding	AUC mean
inferior mediastinal mass	0.9687
intercostal drain	0.9965
internal foreign body	0.9330
kyphosis	0.9642
loculated effusion	0.9523
lower zone bullae	0.9537
lower zone fibrotic volume loss	0.9222
lung collapse	0.9971
lung sutures	0.9657
mastectomy	0.9615
mediastinal clips	0.9929
multifocal airspace opacity	0.8957
multiple masses or nodules	0.9567
neck clips	0.9865
nipple shadow	0.9714
oesophageal stent	0.9980
osteopaenia	0.9431
overexposed	0.9168
patient rotation	0.9092
pectus carinatum	0.8816
pectus excavatum	0.9940
peribronchial cuffing	0.8349
pericardial fat pad	0.9247
perihilar airspace opacity	0.9406
pleural mass	0.9487
pneumomediastinum	0.9689
post resection volume loss	0.9798
pulmonary artery enlargement	0.9416
pulmonary congestion	0.9257
reduced lung markings	0.9539
rib fixation	0.9906
rib lesion	0.9704
rib resection	0.9863
rotator cuff anchor	0.9996

continued

CXR findings (cont.)

Finding	AUC mean
scapular fracture	0.9424
scapular lesion	0.9505
scoliosis	0.9544
segmental collapse	0.9110
shoulder arthritis	0.9830
shoulder dislocation	0.9673
shoulder fixation	0.9969
shoulder replacement	1.0000
simple effusion	0.9510
simple pneumothorax	0.9804
solitary lung mass	0.9462
solitary lung nodule	0.8967
spinal arthritis	0.9243
spinal fixation	0.9992
spinal lesion	0.9710
spinal wedge fracture	0.9501
sternotomy wires	0.9999
subcutaneous emphysema	0.9964
subdiaphragmatic gas	0.9957
suboptimal central line (cvc)	0.9752
suboptimal gastric band	0.9967
suboptimal nasogastric tube (ngt)	0.9848
suboptimal tube (ett)	0.9948
suboptimal pulmonary arterial catheter (pac)	0.9933
superior mediastinal mass	0.9521
tension pneumothorax	0.9973
tracheal deviation	0.9512
underexposed	0.9463
underinflation	0.9726
unfolded aorta	0.8953
upper interstitial thickening	0.8997
upper zone bullae	0.9635
upper zone fibrotic volume loss	0.9763
widened aortic contour	0.9810
widened cardiac silhouette	0.9507

AUC by findings (CTB)

The following tables include all supported findings for Annalise Enterprise (CTB) in alphabetical order. Each row displays both the finding name and the area under the curve (AUC) mean.

These performance results are based on the dataset used by annalise.ai to evaluate the product. Differences in transfer syntax, demographics, imaging equipment or other variables may result in changes in performance.

CTB findings

Finding	AUC mean
Abnormal prominent vessels	0.8478
Acute brainstem infarct	0.8304
Acute cerebellar infarct	0.9279
Acute cerebral infarct	0.9227
Acute haemorrhagic infarct	0.9874
Acute infarct petechial haemorrhage	0.9629
Acute intraparenchymal haemorrhage	0.9853
Acute lacunar infarct	0.8392
Acute on chronic subdural haematoma	0.993
Acute peripheral infarct	0.8879
Acute subdural/extradural haematoma	0.9737
Acute watershed infarct	0.9203
Aggressive bone lesion	0.8865
Aggressive extra-axial mass of soft tissue	0.9786
Aggressive meningeal thickening	0.9127
Aggressive skin lesion	0.9696
Air fluid level paranasal sinuses	0.9481
Aneurysm	0.8111
Aneurysm coils	0.998
Arachnoid cyst	0.9636
Basal ganglia and dentate calcification	0.9699
Cerebellar atrophy	0.9224
Cerebral atrophy	0.8838
Cerebral convexity subarachnoid haemorrhage	0.9658
Chiari malformation	0.9849
Chronic globe abnormality	0.9269
Chronic or fungal sinusitis	0.9693
Chronic subdural haematoma	0.9799

continued

CTB findings (cont.)

Finding	AUC mean
Cochlear implant	0.9999
Colloid cyst	0.998
Colpocephaly	0.9905
Communicating hydrocephalus/NPH	0.9744
Corpus callosum agenesis/hypogenesis	0.9879
Cortical laminar necrosis	0.9415
Cortical or leptomeningeal calcification	0.9523
Craniotomy extra-axial collection	0.9879
Craniotomy/cranioplasty/craniectomy	0.9942
Deep brain stimulation electrodes	1
Deep white or grey matter infarct	0.9483
Diffuse hypoxic-ischaemic encephalopathy	0.9883
Dilated superior opthalmic vein	0.8846
Disappearing basal ganglia sign	0.9562
Dural calcification	0.9478
Effacement of basal cisterns	0.9711
Empty sella	0.95
Encephalomalacia	0.961
Entrapment of lateral ventricle	0.9814
Erosion of bone in tympanic cavity	0.9881
Exophthalmos	0.9699
Expanded pituitary fossa	0.9829
Extracranial herniation	0.953
Extracranial Ventricular Drain (EVD)	0.9939
Extradural haematoma	0.9365
Face and neck haematomas	0.9615
Focal intra-axial calcification	0.9045
Foreign body face and neck	0.9058
Foreign body orbit	0.908
Foreign body scalp	0.8473
Fourth ventricular effacement	0.979
Fracture of calvarium	0.9598
Fracture of skull base	0.9482
Fracture paranasal sinuses/facial bones	0.9348

continued

CTB findings (cont.)

Finding	AUC mean
Generalised calvarial thickening	0.9755
Haemorrhagic contusion	0.9798
Haemorrhagic lesion in sella	0.8986
Hyperdense artery in anterior circulation	0.959
Hyperostosis frontalis	0.9871
Hypopneumatised mastoid	0.9779
Insular ribbon sign	0.9595
Intraaxial lesion calcification	0.9781
Intraaxial lesion complex cyst	0.932
Intraaxial lesion haemorrhage	0.9747
Intraaxial lesion heterogeneous	0.9787
Intraaxial lesion hyperdense	0.961
Intraaxial lesion hypodense	0.9285
Intraaxial lesion isodense	0.9166
Intra-ocular silicone	0.9977
Intra-ventricular haemorrhage	0.9914
Left/Right ventricular effacement	0.9775
Mastoid opacification	0.9073
Mastoidectomy	0.9965
Meningioma with hyperostosis of adjacent calvarium	0.9587
Metallic artefact	0.9688
Midline shift	0.9796
Movement artefact	0.9048
Mucosal thickening	0.9177
Non-aggressive extra-axial mass containing calcification	0.934
Non-aggressive extra-axial mass without calcification or fat	0.8433
Non-aggressive skin lesion	0.8658
Obstructive hydrocephalus	0.981
Old lacunar infarct	0.9151
Opacity in tympanic cavity	0.9866
Orbital fat stranding	0.9539
Orbital mass benign	0.905
Orbital mass inflammatory or malignant	0.9667
Osteoma	0.8637

continued

CTB findings (cont.)

Finding	AUC mean
Parotid lesion	0.8432
Perimesencephalic/aneurysmal subarachnoid haemorrhage	0.9866
Petrous bone fracture	0.9344
Pineal mass or complex cyst	0.8421
Pneumocephalus	0.9393
Prosthetic globe	0.9963
Resection cavity	0.9814
Scalp haematomas	0.9627
Sella or suprasellar cyst, mass or cystic mass	0.9651
Simple pineal cyst	0.9372
Sino-nasal, oral, mandibular and maxillofacial surgery	0.9054
Sinus soft tissue density lesion	0.9299
Small vessel ischaemic disease	0.9375
Soft tissue mass in the neck	0.9058
Striatocapsular slit-like chronic hemorrhage	0.9714
Subacute intraparenchymal haemorrhage	0.9249
Subacute subdural haematoma	0.9788
Subcutaneous emphysema	0.9358
Subependymal calcification or nodules	0.8622
Sulcal effacement	0.9654
Temporomandibular joint arthritis	0.8514
Temporomandibular joint dislocation	0.9691
Third ventricular effacement	0.9843
Tonsillar herniation	0.9933
Transependymal oedema	0.9814
Transphenoidal surgery	0.9569
Uncal herniation	0.9927
Vascular clips	0.9839
Vasogenic oedema	0.9765
Ventricular cyst/xanthogranulomatous change	0.8713
Ventricular mass	0.8212
Ventriculoperitoneal (VP) Shunt	0.9975
Vitreous haemorrhage	0.9741

Model validation dataset characteristics

Dataset characteristics (CXR)

The Annalise Enterprise product is validated on over 2,500 studies (both lossless transfer syntax and lossy transfer syntax) acquired from clinics across Australia and the United States of America.

Demographics of the overall test dataset:

- Patients: 2286
- Studies: 2568
- Images: 4568
- Sex: 29% male, 28% female, 43% unknown*
- Mean Age: 74 years, (standard deviation 15 years)*
- View Position: 28% posterior-anterior (PA), 33% anterior-posterior (AP), 31% optionally lateral (LAT), 8% other

*As MIMIC-CXR does not provide sex or age information, data for this is incomplete.

Dataset of origin

Dataset of origin of images were obtained from I-MED and the publicly available MIMIC dataset.

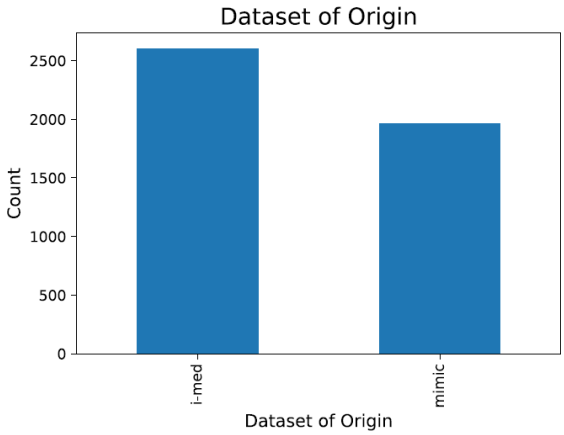

Patient age

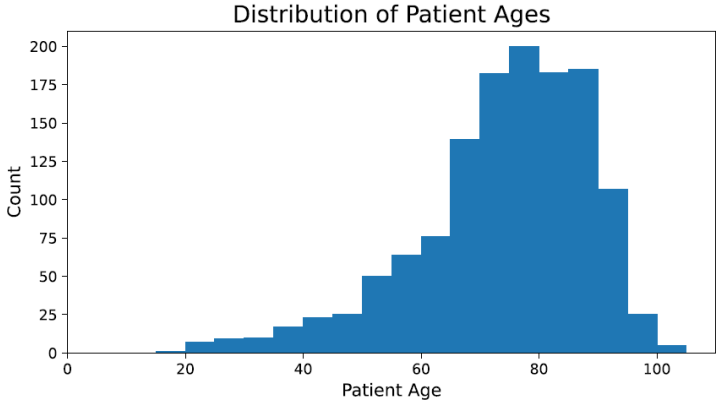

Patient sex

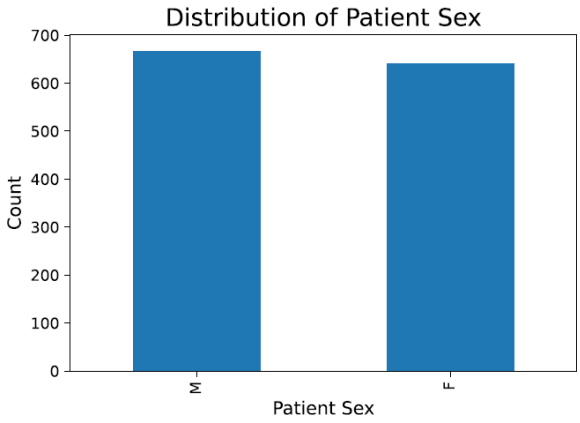

View/position characteristics

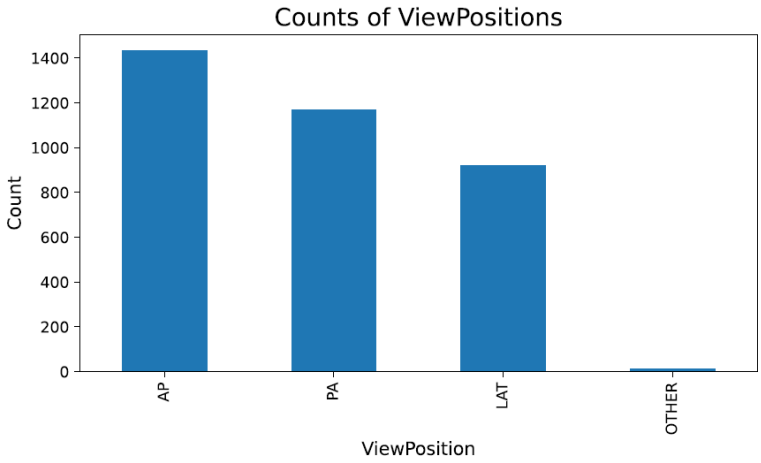

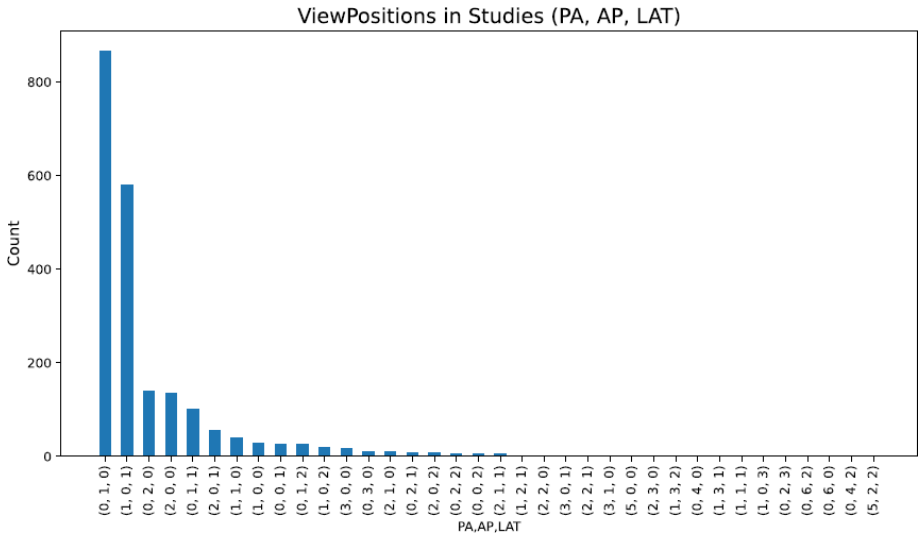

Dataset characteristics (CTB)

The Annalise Enterprise product is validated on over 2,500 studies (lossless transfer syntax) acquired from a single Australian source (I-MED Radiology Network Limited).

The test dataset comprised 2,848 studies originating from 2,419 unique patients from a single Australian source (I-MED Radiology Network Limited).

Mean patient age was 63.9 years (standard deviation 18.2).

Distribution of patient sex was 1,524 male (53.5%), 1,322 female (46.4%) and 2 undisclosed.

Patient age

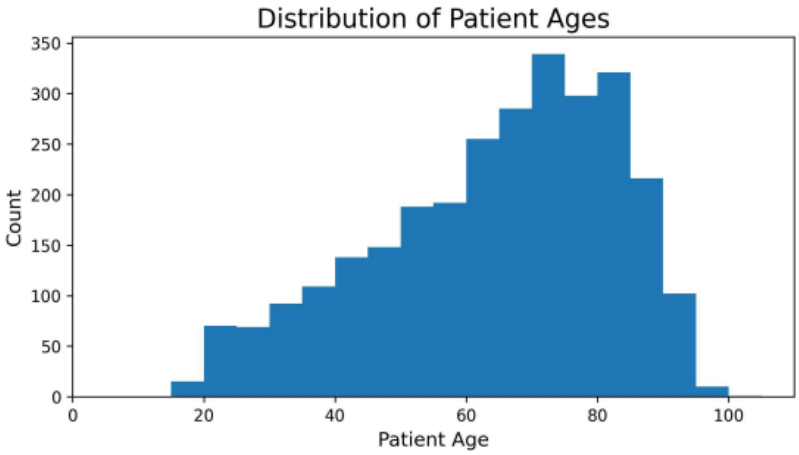

Patient sex

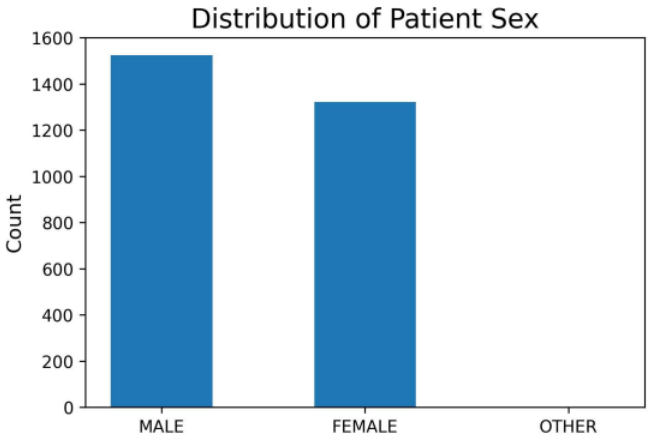

Acquisition modality of images (CXR)

Overview

The Acquisition Modality is an important marker of image quality.

Computed Radiography (CR) is an older technology which records information on a phosphor cassette prior to digitisation, while Digital Radiography (DX) records and digitises information at the detector, leading to improved spatial resolution.

Decreased spatial resolution may lead to difficulty in distinguishing fine detail on X-rays (such as rib fractures or lung nodules).

Acquisition modality

The following graph displays the distribution of acquisition modalities:

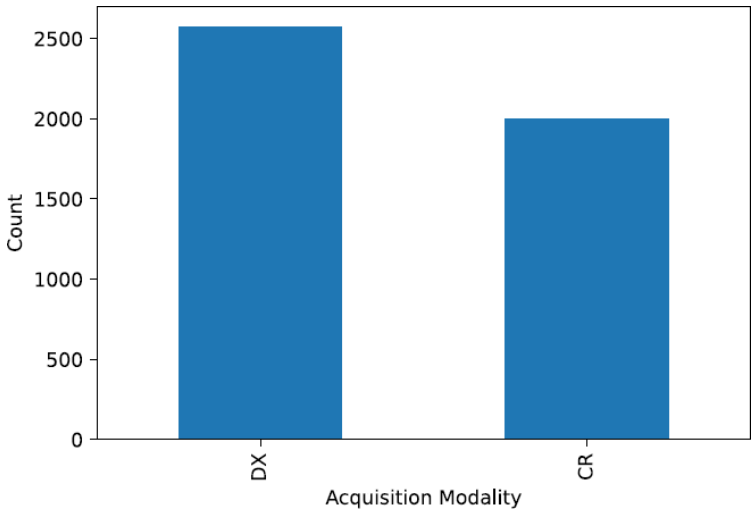

Imaging device

Overview

This section outlines the distribution characteristics of:

- detector type (CXR)
- imaging device manufacturers (CXR and CTB)
- imaging device models (CXR and CTB)

Detector type (CXR)

When digital radiography is used, the type of detector also changes the image quality.

Scintillator detectors are older technologies which convert X-ray photons to visible photons via scintillation crystals, while direct detectors detect X-ray photons without an intermediate step.

Direct detectors tend to have improved modulation transfer function and spatial resolution. Decreased spatial resolution may lead to difficulty in distinguishing fine detail on X-rays (such as rib fractures or lung nodules).

The following graph displays the distribution of detector types of radiographs:

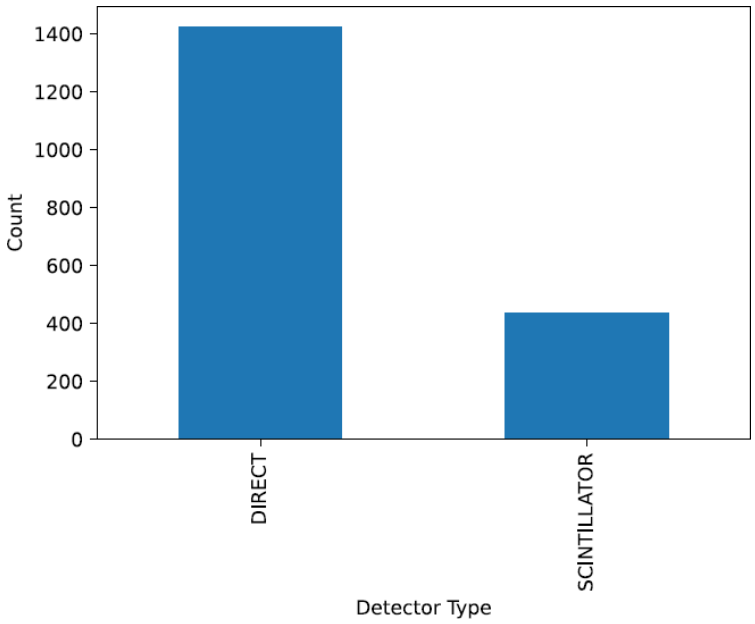

Imaging device models and manufacturers (CXR)

The following graphs display the distribution of CXR imaging device models and manufacturers:

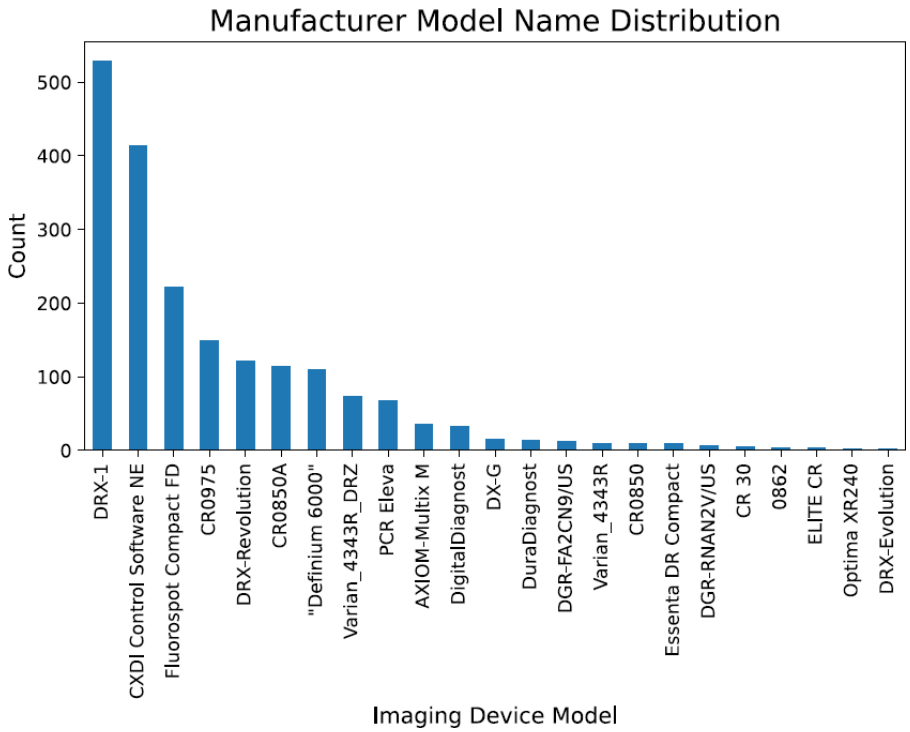

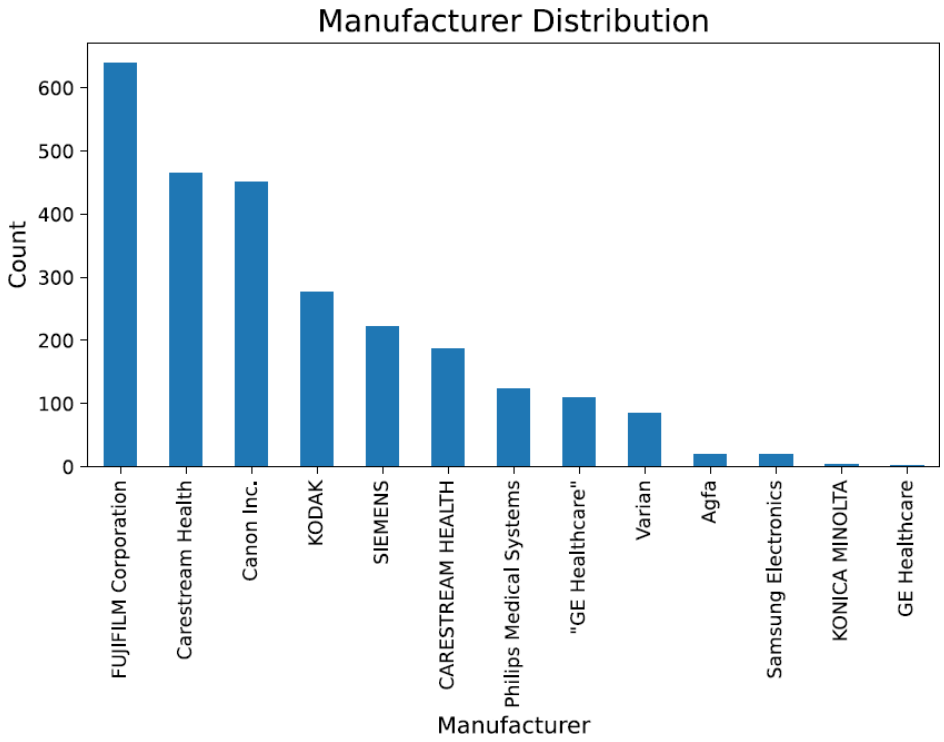

Imaging device models and manufacturers (CTB)

The following graphs display the distribution of CTB imaging device models and manufacturers:

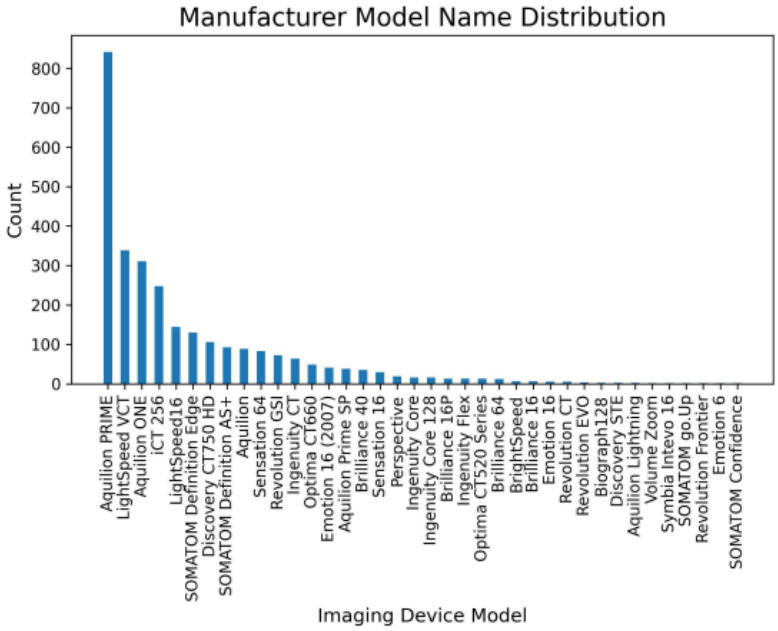

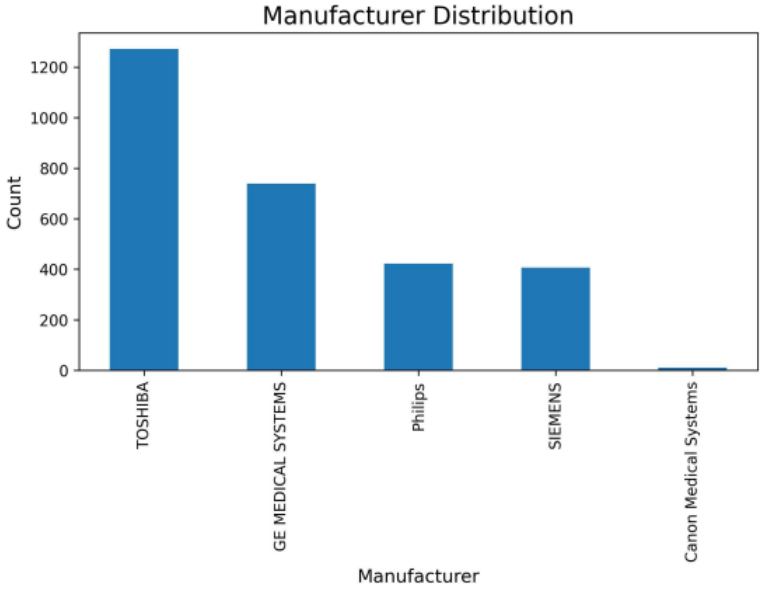

Distribution of peak kV (CXR)

Overview

The peak kilovolt (KVP) is selected by the radiographer at the time of imaging and can affect image quality.

With automatic exposure control in most systems, higher KVP leads to more X-rays passing through the body and reaching the detector, reducing dose but also reducing contrast resolution.

Lower KVP improves contrast resolution but increases dose to the patient. Too high KVP may lead to difficulty in distinguishing low contrast structures like lung opacities.

Results

The following graphs display the peak voltage in kV for frontal and lateral views:

Frontal views

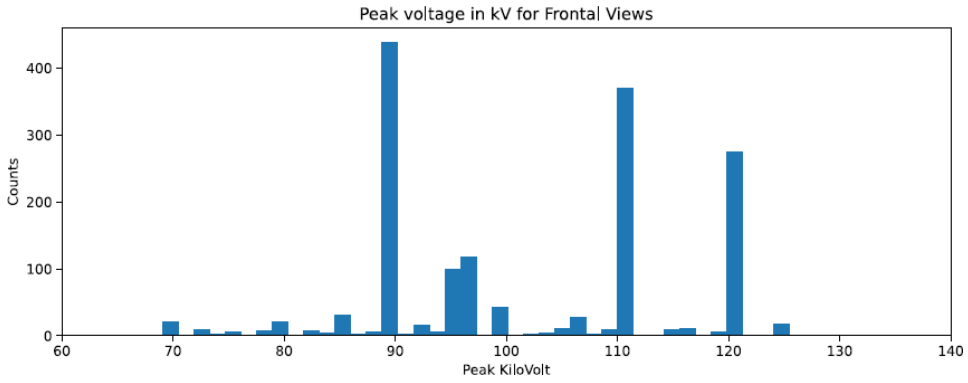

Lateral views

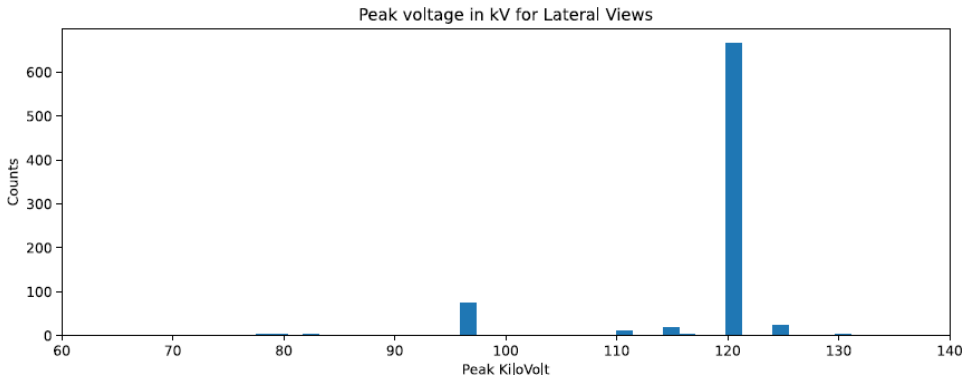

Distribution of exposure in uAs (CXR)

Overview

The exposure in micro-ampere-seconds (uAs) is the total output of the X-ray tube and is usually automatically controlled by using automatic exposure control. This aims to maintain image quality while reducing exposure as low as reasonably achievable.

Therefore, lateral views will require more exposure where there is more tissue for the X-ray photons to pass through.

Changing the exposure manually will change the Exposure Index (EI) and Deviation Index (DI).

Results

The following graphs display the exposure in uAs for frontal and lateral views:

Frontal views

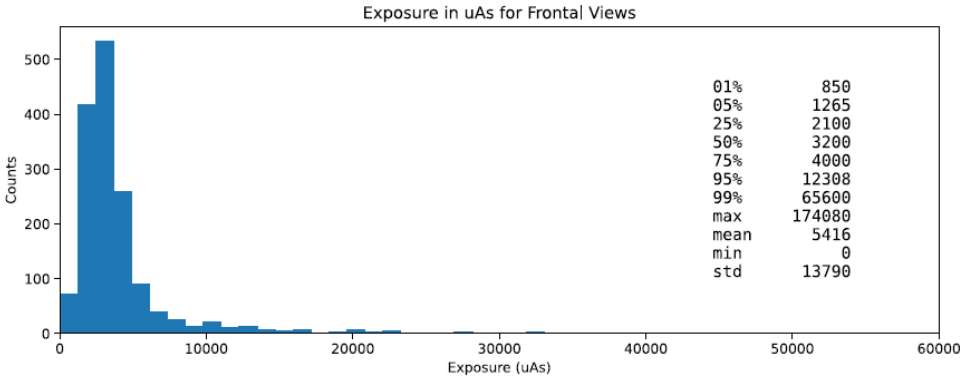

Lateral views

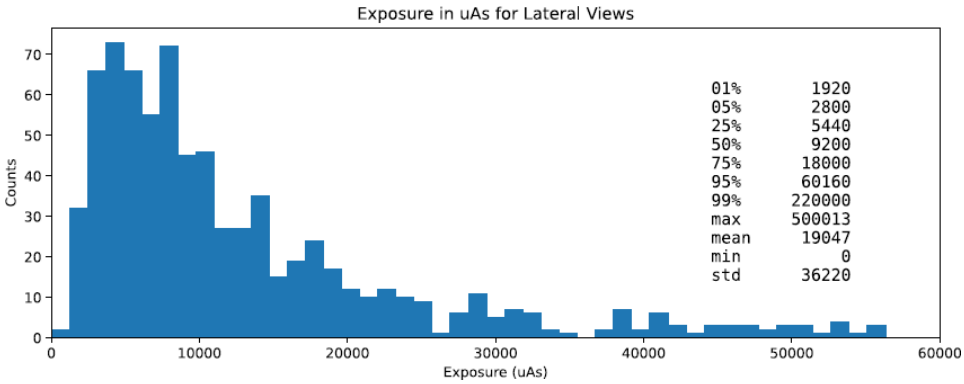

Radiograph quality indices (CXR)

Overview

The Exposure Index (EI) is a measure of the incident radiation on the detector plate. When automatic exposure control (AEC) is used, it should be roughly similar within the same exam type (for example, frontal chest radiographs) as AEC aims to maintain exposure at a target exposure index.

The Deviation Index (DI) is a logarithmic measure of the difference between the target exposure index and the actual target exposure. High deviation index indicates overexposure while low deviation index indicates underexposure (likely to cause the image to appear more white than necessary).

Different EIs and DIs may lead to difficulty in visualising structures with poor contrast resolution (such as lung opacities).

Results

The following graphs display the exposure index for frontal and lateral views and the deviation index for frontal and lateral views:

Exposure index for frontal views

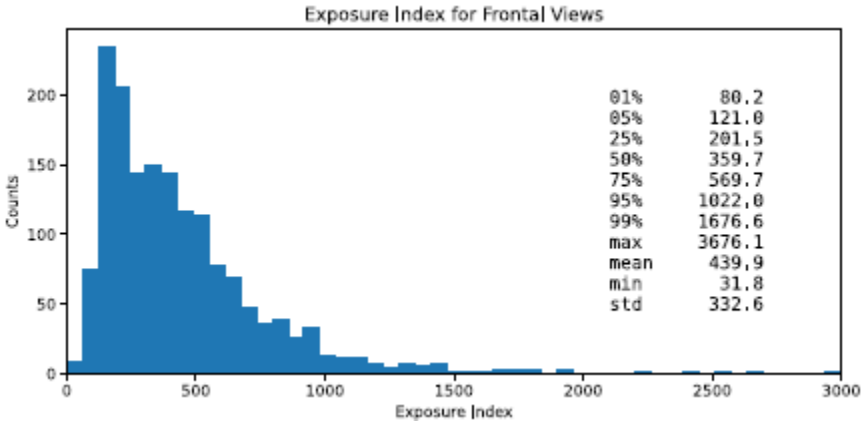

Exposure index for lateral views

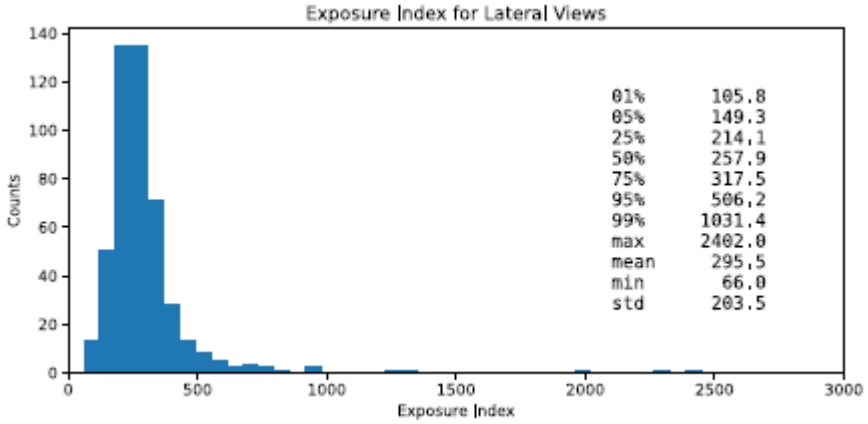

Deviation index for frontal views

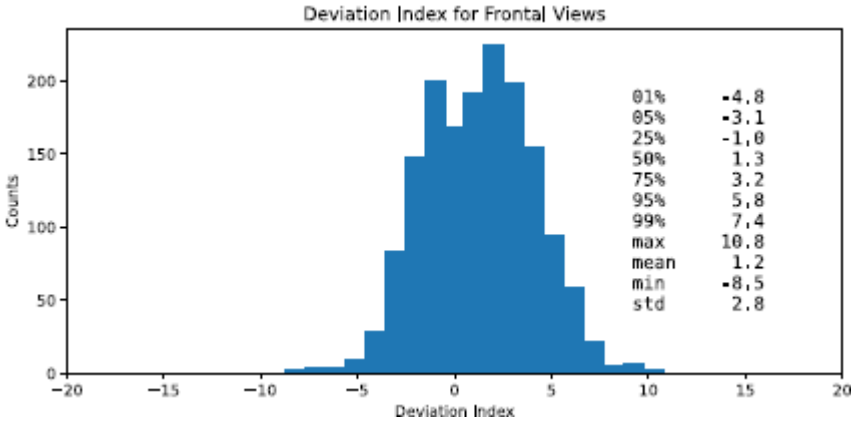

Deviation index for lateral views

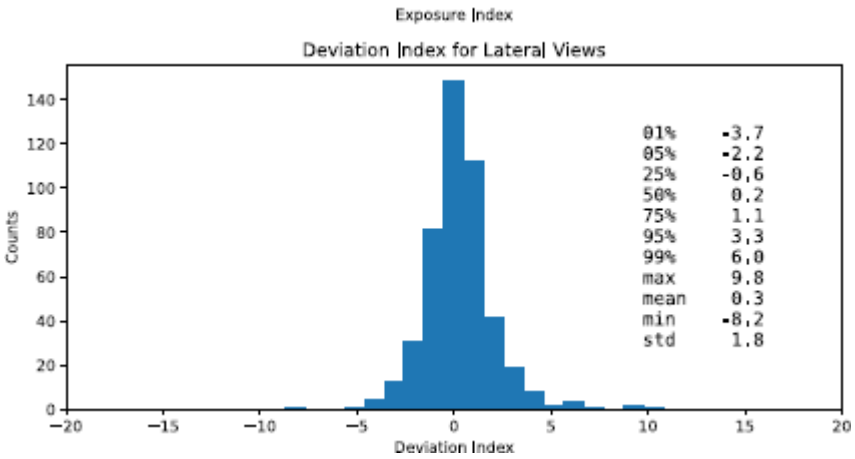

Pixel spacing values

Overview

Pixel spacing is the measure of the physical distance between each recorded pixel on the detector. It is not adjusted for geometric magnification.

Higher pixel spacing values typically indicate improved spatial resolution unless post-processing has been applied to the image.

Decreased spatial resolution may lead to difficulty in distinguishing fine detail on X-rays (such as rib fractures or lung nodules) and CT scans (such as subtle bleeds and fractures).

Pixel spacing values (CXR)

The following graph displays the pixel spacing values for cases in the dataset:

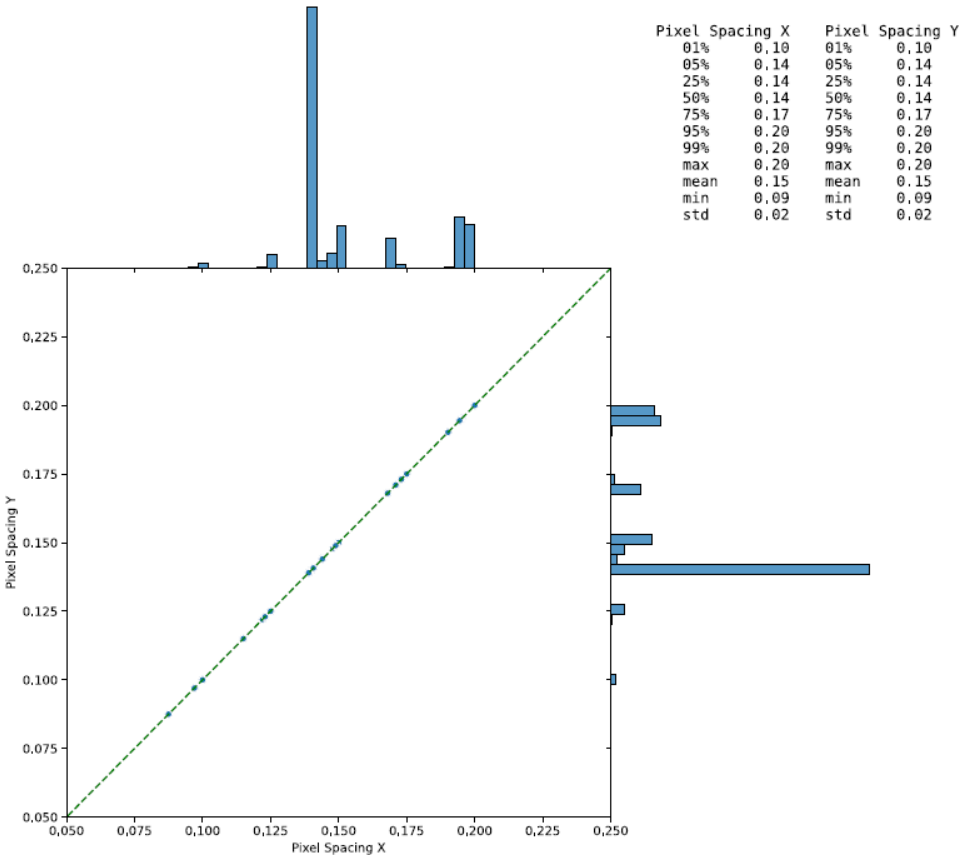

Pixel spacing values (CTB)

Distribution of pixel spacing ranged from 0.65 mm (max) to 0.31 mm (min) with a mean of 0.43 mm across all images (standard deviation 0.03).

The following graph displays the pixel spacing values for the cases in the dataset:

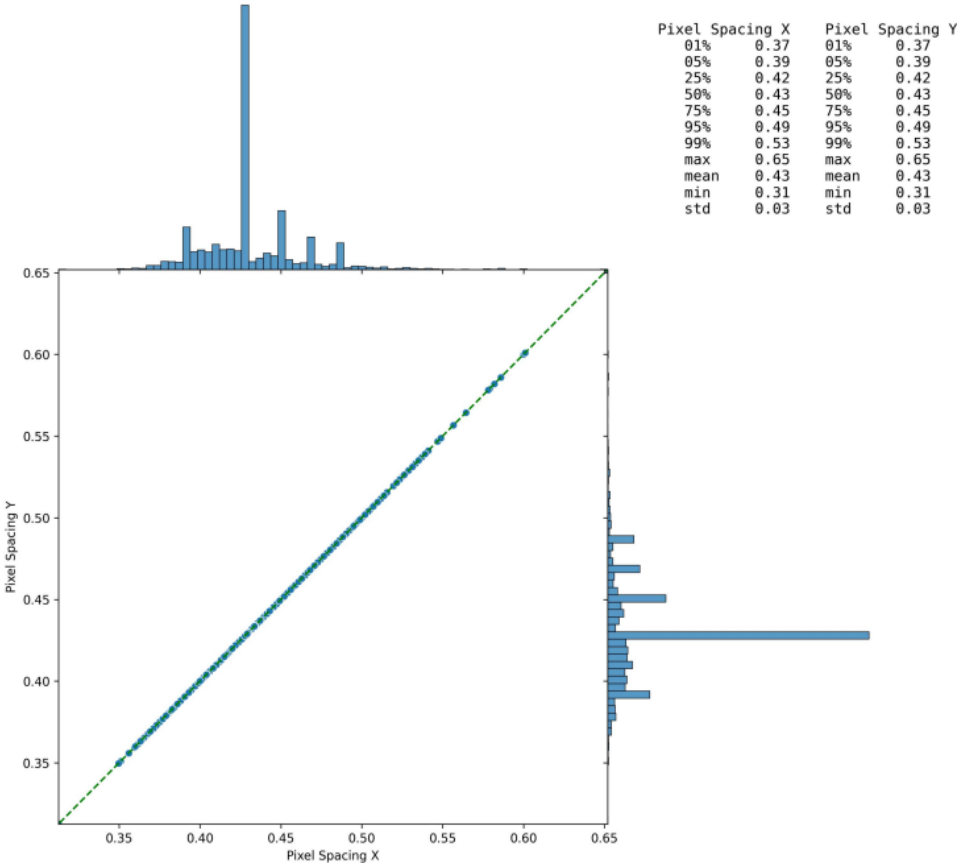

ANNALISE-AI PTY LTD,
Level 21, 60 Margaret Street,
Sydney, NSW 2000
AUSTRALIA

ABN: 92 635 645 260

ANNALISE-AI UK LTD, 100 New Bridge Street,
London, EC4V 6JA
ENGLAND

Company no: 12804340

support@annalise.ai
www.annalise.ai

OPT-PRM-029 Ver.0